

Supporting Information for: Variation from Closed-Shell to Open Shell Electronic Structures in Oligothiophene Bis(dioxolene) Complexes

Paul D. Miller,¹ David A. Shultz,^{*1} Joshua Mengell,² Martin L. Kirk,^{*2,3,4} and Lukasz Wojtas⁵

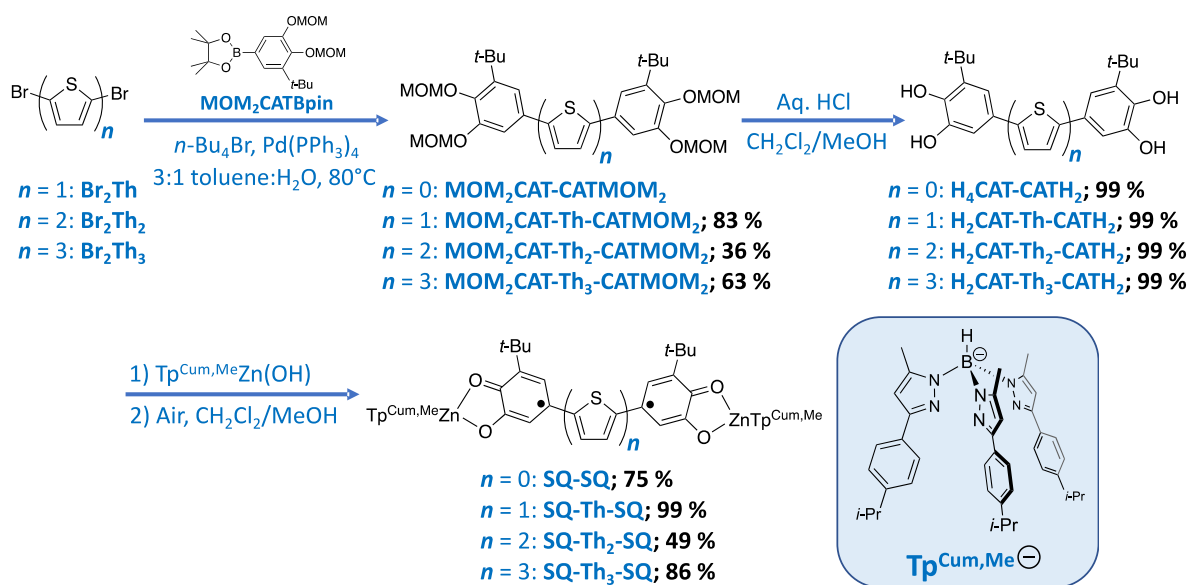
Table of Contents

General Experimental	S1
Synthesis	S1
EPR Spectroscopy	S5
Magnetic Susceptibility Experiments	S6
Electronic Absorption Spectroscopy	S6
X-Ray Crystallography	S6
¹ H NMR Comparison of SQ ₂ Th and SQ ₂ Th ₂	S14

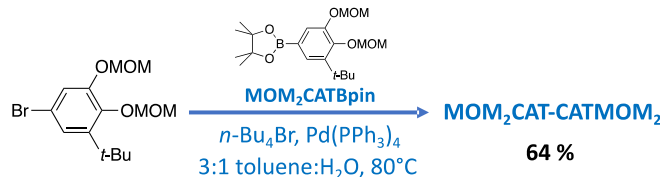
General. All chemical reagents were purchased and used as received. Anhydrous and/or degassed solvents were obtained by drying solvent over sieves and purging with nitrogen. MOM₂CatBpin¹ and Cum,MeTpZn(OH)² were synthesized according to literature methods. NMR Spectra were recorded on Bruker-400 and Variant-400 spectrometers. Mass spectra were recorded using *Thermo Fisher Scientific Exactive Plus MS*. Absorption spectra were recorded on a Hitachi U-4100 Spectrometer. An Oxford Instruments Optistat CF cryostat was used for all VT-EAS experiments. SQUID magnetometry was performed using a Quantum Design MPMS[®]3 magnetometer with SQUID detection. EPR experiments were conducted on a Bruker X-band EPR.

Synthesis. The synthetic scheme for SQ-Th_n-SQ (n = 0-3) complexes is shown in Scheme S1.

Scheme S1. Synthesis of Bis(semiquinone) Biradicals.



Scheme S1. Continued.



3,3'-Di-*tert*-butyl-4,4',5,5'-tetrakis(methoxymethyl)-1,1'-biphenyl (MOM₂Cat-CatMOM₂).

MOM₂CatBr (132 mg, 0.395 mmol), MOM₂CatBpin (150 mg, 0.395 mmol), Na₂CO₃ (84 mg, 0.790 mmol), and TBAB (13 mg, 0.04 mmol) were added to a 50 mL RBF equipped with a stir bar. In a glovebox, Pd(PPh₃)₄ (5 mg, 0.004 mmol) was added to the RBF. Outside the glovebox, 15 mL of dry, degassed toluene and 5 mL of deoxygenated water were added to the flask, a nitrogen flushed condenser was attached, and the reaction was heated to 80 °C and stirred for 16 hours. The reaction was then cooled to room temperature, diluted with Et₂O, and washed with H₂O and brine. The organic phase was isolated and dried over MgSO₄. The organic phase was then filtered and concentrated to yield the crude product which was subsequently purified via column chromatography [Hexanes/Et₂O [3:1], silica; deactivated with 1% TEA in hexanes; product R_f = 0.2] to yield **MOM₂Cat-CatMOM₂** (127 mg, 64%) as a clear oil. ¹H NMR (400 MHz, CD₂Cl₂) δ = 7.14 (s, 4 H), 5.22 (s, 8 H), 3.68 - 3.61 (m, 6 H), 3.55 - 3.47 (m, 6 H), 1.45 (s, 18 H). ¹³C NMR (101 MHz, CD₂Cl₂) δ = 150.8, 146.1, 144.1, 136.9, 120.0, 114.4, 99.7, 96.2, 58.0, 56.8, 35.8, 30.9; HRMS (TOF MS ES+) *m/z*: [M+H]⁺ calcd for [C₂₈H₄₃O₈]⁺ 507.2958, found 507.2943.

5,5'-Di-*tert*-butyl-[1,1'-biphenyl]-3,3',4,4'-tetraol (H₄Cat-CatH₄).

MOM₂Cat-CatMOM₂ (55 mg, 0.11 mmol) was dissolved in minimal MeOH in a 10 mL μ-wave vial. Two drops of 4 M HCl were added to the vial, which was then capped with a pressure cap and placed in the microwave reactor. The reaction was heated to 90 °C for 5 minutes, then immediately cooled to room temperature with air flow. The solution was then concentrated with Et₂O trituration to yield **H₄Cat-CatH₄** (36 mg, 99%) as a solid. The material was immediately carried over to the next step.

SQ-SQ (SQ₂).

H₄Cat-CatH₄ (36 mg, 0.11 mmol) and Tp^{Cum,Me}Zn(OH) (150 mg, 0.217 mmol) were degassed with N₂ in a 50 mL RBF. The solids were then dissolved by N₂ sparged CH₂Cl₂/MeOH (1:1) [16 mL] and stirred under N₂ for 15 minutes. The reaction was opened then to air and stirred overnight. The reaction was then concentrated and filtered to isolate a precipitate which was washed with MeOH to yield **SQ-SQ** (150 mg, 75%) as a green solid. X-ray quality crystals were grown in CH₂Cl₂ layered in MeOH. HRMS (FTMS + pESI) *m/z*: [M+2H]²⁺ calcd for [C₉₈H₁₁₄B₂N₁₂O₄Zn₂]²⁺ 842.3963, found 842.3991.

2,5-Bis(3-(*tert*-butyl)-4,5-bis(methoxymethoxy)phenyl)thiophene (MOM₂CAT-Th-CATMOM₂).

2,5-Dibromothiophene (215 mg/0.100 mL, 0.887 mmol), MOM₂CatBpin (709 mg, 1.864 mmol), Na₂CO₃ (376 mg, 3.548 mmol), and tetrabutylammonium bromide (29 mg, 0.09 mmol) were added to an oven dried 50 mL Schlenk flask equipped with a stir bar. The solids were degassed under vacuum and kept under a nitrogen atmosphere. In a glovebox, Pd(PPh₃)₄ (10 mg, 0.009 mmol) was added to the RBF. Outside the glovebox, 15 mL of dry, degassed toluene and 5 mL of deoxygenated water were added to the flask, a nitrogen flushed condenser was attached, and the reaction was heated to 80 °C and stirred for

48 hours. The reaction was then cooled to room temperature, diluted with Et₂O, and washed with brine. The organic phase was isolated and dried over sodium sulfate. The organic phase was then filtered and concentrated to yield the crude product which was subsequently purified via column chromatography [Hexanes/EtOAc (6:1), silica; deactivated with 1% TEA in hexanes] to yield **MOM₂CAT-Th-CATMOM₂** (456 mg, 87%) as a yellow oil. ¹H NMR (400 MHz, CDCl₃) δ = 7.28 (d, J = 2.2 Hz, 2 H), 7.27 (d, J = 2.2 Hz, 2 H), 7.17 (s, 2 H), 5.25 (s, 4 H), 5.24 (s, 4 H), 3.68 (s, 6 H), 3.56 (s, 6 H), 1.48 (s, 18 H). ¹³C NMR (101 MHz, CDCl₃) = 150.4, 145.6, 143.8, 143.4, 129.5, 123.6, 118.3, 112.0, 99.1, 95.5, 57.6, 56.4, 35.3, 30.5; HRMS (TOF MS ES⁺) *m/z*: [M+H]⁺ calcd for [C₃₂H₄₅O₈S]⁺ 589.2835, found 589.2820.

5,5'-(Thiophene-2,5-diyl)bis(3-(*tert*-butyl)benzene-1,2-diol) (H₂CAT-Th-CATH₂). **MOM₂CAT-Th-CATMOM₂** was transferred to a 50 mL RBF, degassed and kept under nitrogen, then redissolved in 15 mL of dry CH₂Cl₂/MeOH (2:1). 1 mL of concentrated HCl was added via syringe and the reaction was stirred overnight. Degassed water was added to reaction via syringe and removed via syringe after stirring for 15 minutes. Sodium sulfate was quickly added to the reaction vessel, and the organic phase was transferred to another RBF via canula filtration. Solvent was removed via high vac to yield **H₂CAT-Th-CATH₂** (154 mg, 99%) as a blue solid. Material was immediately carried over into the next reaction.

2,5-SQ₂-Thiophene (SQ-Th-SQ). **H₂CAT-Th-CATH₂** (37 mg, 0.090 mmol), Zn(OH)Tp^{Cum,Me} (127 mg, 0.184 mmol), and K₂CO₃ (25 mg, 0.180 mmol) were added to an oven dried round bottom flask and purge pumped three times. The solids were dissolved in 10 mL of CH₂Cl₂ and 5 mL of MeOH then the solution was left to stir under a nitrogen atmosphere for 24 h. The reaction was then opened to air and left to stir for another 24 h. The resulting suspension was further dried via rotary evaporation, suspended in MeOH, and the precipitate was isolated via filtration. The solid was washed with MeOH and collected with CH₂Cl₂, then concentrated under reduced pressure and recrystallized via vapor diffusion of EtOH and CH₂Cl₂ to afford **SQ₂Th** (157 mg, 99%) as a purple solid. X-ray quality single crystals were grown by dissolving SQ₂Th in CH₂Cl₂ and layering with isopropanol then allowing for slow diffusion to occur. HRMS (TOF MS ES⁺) *m/z*: [M+H]⁺ calcd for [C₁₀₂H₁₁₇B₂N₁₂O₄SZn₂]⁺ 1753.7883, found 1753.7904.

5,5'-Bis(3-(*tert*-butyl)-4,5-bis(methoxymethoxy)phenyl)-2,2'-bithiophene (MOM₂CAT-Th₂-CATMOM₂). 5,5'-Dibromo-2,2'-bithiophene (180 mg, 0.745 mmol), MOM₂CatBpin (595 mg, 1.565 mmol), Na₂CO₃ (316 mg, 2.98 mmol), and TBAB (24 mg, 0.075 mmol) were added to a 50 mL RBF equipped with a stir bar. In a glovebox, Pd(PPh₃)₄ (9 mg, 0.008 mmol) was added to the RBF. Outside the glovebox, 15 mL of dry, degassed toluene and 5 mL of deoxygenated water were added to the flask, a nitrogen flushed condenser was attached, and the reaction was heated to 80 °C and stirred for 48 hours. The reaction was then cooled to room temperature, diluted with Et₂O, and washed with brine. The organic phase was isolated and dried over sodium sulfate. The organic phase was then filtered and concentrated to yield the crude product which was subsequently purified via column chromatography [Hexanes/EtOAc (5:1), silica; deactivated with 1% TEA in hexanes] to yield the desired compound (376 mg, 75%) as a bright yellow solid. ¹H NMR (400 MHz, CDCl₃) δ = 7.28 (d, J = 2.1 Hz, 2 H), 7.25 (d, J = 2.1 Hz, 2 H), 7.15 (d, J = 3.8 Hz, 2 H), 7.14 (d, J = 3.8 Hz, 2 H), 5.24 (s, 8 H), 3.68 (s, 6 H), 3.56 (s, 6 H), 1.48 (s, 18 H). ¹³C NMR (101 MHz, CDCl₃) δ = 150.5, 145.8, 143.9, 143.2, 136.4, 129.1, 124.2, 123.4, 118.3, 112.1, 99.1, 95.5, 57.6, 56.4, 35.3, 30.5; HRMS (TOF MS ES⁺) *m/z*: [M+H]⁺ calcd for [C₃₆H₄₆O₈S₂]⁺ 670.2634, found 670.2629.

5,5'-([2,2'-Bithiophene]-5,5'-diyl)bis(3-(*tert*-butyl)benzene-1,2-diol) (H₂CAT-Th₂-CATH₂). **MOM₂CAT-Th₂-CATMOM₂** (93 mg, 0.14 mmol) was transferred to a 50 mL RBF, degassed and kept under nitrogen, then redissolved in 25 mL of dry CH₂Cl₂/MeOH (3:2). 2 mL of concentrated HCl was added via syringe and the reaction was stirred overnight. The next day the reaction was diluted with Et₂O, washed

with brine, dried over sodium sulfate, and concentrated under reduced pressure to afford **H₂CAT-Th-CATH₂** (69 mg, 99%) as a dark yellow solid. Material was immediately carried over into the next reaction.

5,5'-SQ₂-Bithiophene (SQ-Th₂-SQ). **H₂CAT-Th₂-CATH₂** (69 mg, 0.14 mmol), Zn(OH)Tp^{Cum,Me} (197 mg, 0.29 mmol), and K₂CO₃ (38 mg, 0.278 mmol) were added to an oven dried round bottom flask and purge pumped three times. The solids were dissolved in 10 mL of CH₂Cl₂ and 5 mL of MeOH then the solution was left to stir under a nitrogen atmosphere for 24 h. The reaction was then opened to air and left to stir for another 24 h. The resulting suspension was further dried via rotary evaporation, slurried in MeOH, then the precipitate was isolated via filtration. The solid was washed with MeOH and collected with CH₂Cl₂, then concentrated under reduced pressure to afford **SQ-Th₂-SQ** (126 mg, 49%) as a dark green solid. X-ray quality crystals were grown in CH₂Cl₂ layered with EtOH. HRMS (TOF MS, ES⁺) *m/z*: [M+H]⁺ calcd for [C₁₀₆H₁₁₉B₂N₁₂O₄S₂Zn₂]⁺ 1835.7760, found 1835.7644.

5,5''-Bis(3-(*tert*-butyl)-4,5-bis(methoxymethoxy)phenyl)-2,2':5',2''-terthiophene (MOM₂CAT-Th₃-CATMOM₂). 5,5''-Dibromoterthiophene (270 mg, 0.664 mmol), MOM₂CatBpin (530 mg, 1.394 mmol), Na₂CO₃ (282 mg, 2.656 mmol), and tetrabutylammonium bromide (23 mg, 0.07 mmol) were added to an oven dried 50 mL Schlenk flask equipped with a stir bar. The solids were degassed under vacuum and kept under a nitrogen atmosphere. In a glovebox, Pd(PPh₃)₄ (8 mg, 0.007 mmol) was added to the RBF. Outside the glovebox, 15 mL of dry, degassed toluene and 5 mL of deoxygenated water were added to the flask, a nitrogen flushed condenser was attached, and the reaction was heated to 80 °C and stirred for 48 hours. The reaction was then cooled to room temperature, diluted with Et₂O, and washed with brine. The organic phase was isolated and dried over sodium sulfate. The organic phase was then filtered and concentrated to yield the crude product which was subsequently purified via column chromatography (Hexanes/EtOAc (4:1), silica; deactivated with 1% TEA in hexanes) to yield 10 (440 mg, 88%) as an orange solid. ¹H NMR (400 MHz, CDCl₃) δ = 7.29 - 7.27 (d, J = 2.1 Hz, 2 H), 7.25 (d, J = 2.1 Hz, 2 H), 7.17 - 7.12 (m, 4 H), 7.11 (s, 2 H), 5.24 (s, 8 H), 3.68 (s, 6 H), 3.56 (s, 6 H), 1.47 (s, 18 H); ¹³C NMR (101 MHz, CDCl₃) δ = 150.5, 145.8, 143.9, 143.4, 136.1, 135.9, 129.0, 124.4, 124.1, 123.5, 118.2, 112.0, 99.1, 95.5, 77.4, 77.1, 76.7, 57.6, 56.4, 35.3, 35.1, 30.5, 30.4, 24.8; HRMS (TOF MS, ES⁺) *m/z*: [M+H]⁺ calcd for [C₄₀H₄₉O₈S₃]⁺ 753.2590, found 753.2554.

5,5'-([2,2':5',2''-Terthiophene]-5,5''-diyl)bis(3-(*tert*-butyl)benzene-1,2-diol) (H₂CAT-Th₃-CATH₂). MOM₂CAT-Th₃-CATMOM₂ (315 mg; 0.418 mmol) was transferred to a 50 mL RBF, degassed and kept under nitrogen, then dissolved in 25 mL of dry CH₂Cl₂/MeOH (3:2). HCl (2 mL) was added via syringe and the reaction was stirred overnight. The next day the reaction was diluted with Et₂O, washed with brine, dried over sodium sulfate, and concentrated under reduced pressure to afford **H₂CAT-Th₃-CATH₂** (235 mg, 99%) as a dark yellow solid. Material was immediately carried over into the next reaction.

5,5''-SQ₂-Terthiophene (SQ-Th₃-SQ). **H₂CAT-Th₃-CATH₂** (79 mg, 0.141 mmol), Zn(OH)Tp^{Cum,Me} (195 mg, 0.282 mmol), and K₂CO₃ (195 mg, 0.282 mmol) were added to an oven dried round bottom flask and purge pumped three times. The solids were dissolved in 15 mL of CH₂Cl₂ and 5 mL of MeOH then the solution was left to stir under a nitrogen atmosphere for 24 h. The reaction was then opened to air and left to stir for another 24 h. The resulting suspension was further dried via rotary evaporation, slurried in MeOH, then the precipitate was isolated via filtration. The solid was washed with MeOH to afford pure **SQ-Th₃-SQ** (232 mg, 86%) as a dark red solid. X-ray quality crystals were grown in chloroform layered with MeOH. HRMS (TOF MS, ES⁺) *m/z*: [M+2H]²⁺ calcd for [C₁₁₀H₁₂₂B₂N₁₂O₄S₃Zn₂]²⁺ 1918.7716, found 1918.7524.

Electron Paramagnetic Resonance Spectroscopy. EPR spectra were recorded on a Brüker ELEXSYS-II E500 CW EPR spectrometer with low temperature capabilities. For SQ₂Th₃, ca. 2 mM in biradical (frozen solution experiments) were prepared in freshly distilled 2-methyl-tetrahydrofuran, degassed, and the spectra collected in quartz EPR tubes. For SQ₂Th₂, ca. 2 mM solution of biradical was made in a saturated solution of poly(vinyl)chloride in CH₂Cl₂. This biradical/polymer solution was pipetted onto a glass surface evenly, then covered with a watch glass to allow for slow evaporation. The resulting biradical infused polymer film was used for all SQ₂Th₂ EPR experiments.

All triplet powder spectra collected with fit utilizing EasySpin, a computational EPR package based in MatLab.³ See below Tables E1 and E2 for the fitting parameters used to fit SQ₂Th₂ and SQ₂Th₃ powder spectra, respectively.

Table E1: SQ₂Th₂ EasySpin Fitting Parameters		
Parameter	Doublet Impurity	Triplet
g_x	2.0049	2.0056
g_y	2.0049	2.0030
g_z	2.0049	2.0073
Line Width (Gaussian)	0.08	0.16
Line Width (Lorentzian)	0.97	0.76
Weight	0.34	0.66
D [cm ⁻¹]	-	0.0058
E [cm ⁻¹]	-	0.0009
g_x Strain	-	2.40E-06
g_y Strain	-	0.0128
g_z Strain	-	0.0140

Table E2: SQ₂Th₃ EasySpin Fitting Parameters		
Parameter	Doublet Impurity	Triplet
g_x	2.0058	2.0055
g_y	2.0036	2.0029
g_z	2.0057	2.0061
Line Width (Gaussian)	0.51	0.51
Line Width (Lorentzian)	0.16	0.0043
Weight	0.36	0.64
D [cm ⁻¹]	-	0.00342
E [cm ⁻¹]	-	0.00062
g_x Strain	-	0
g_y Strain	-	0.0025
g_z Strain	-	0.0043

Magnetic Susceptibility and Magnetization Measurements. Magnetic susceptibility measurements were collected on a Quantum Design MPMS-XL7 SQUID magnetometer with an applied field of 0.7 T. A crystalline sample (~20 mg) was loaded into a gel cap/straw sample holder and mounted to the sample rod with Kapton tape for variable temperature measurements. Raw data were corrected with Pascal's constants as a first approximation for molecular diamagnetism followed by a straight line correction to all data for the diamagnetic response of sample container where the slope of the line represents the residual diamagnetic correction. The magnetic susceptibility data were fit using a field-independent van Vleck

expression, $\chi_{\text{eff}}T = [\chi/(1-\theta\chi)]T$, where $\theta = \frac{2zJ'_{\text{inter}}}{Ng^2\beta^2}$, and $\chi = \frac{0.75g^2}{3 + \exp\left(\frac{-2J_{\text{SQ}} - sQ}{0.695 \cdot T}\right)}$, and J_{SQSQ} is the SQ-Bridge-SQ magnetic exchange parameter.⁴ The origin of zJ'_{inter} may be zero-field splitting, intermolecular interactions, saturation effects, or some combination of all three.^{4,5} In our data, the effects of zJ'_{inter} are negligible compared to $J_{\text{SQ-B-SQ}}$, and varying results in 10-15% changes in $J_{\text{SQ-B-SQ}}$, which is insufficient to alter either our discussion or conclusions. In fact, by omitting the $\chi_{\text{para}} \cdot T$ data points below 10K, the data can be fit adequately without the zJ'_{inter} term. Typically, the small deviation of the g -values (as a fit parameter) from the expected spin-only value of ~2.00 can be the result of minute (~1%) weighing errors. We note that excellent fits could be obtained without including any "J-strain," which suggests that thermal (de)population of vibrational/torsional levels has no effect on the magnetic data, in accord with our published results on other SQ-Bridge-NN molecules. Finally, shown below in **Figure S1** is the SQUID data collected for **SQ₂Th** on a crystalline sample, which possesses diamagnetic properties between 5 to 300 K by SQUID.

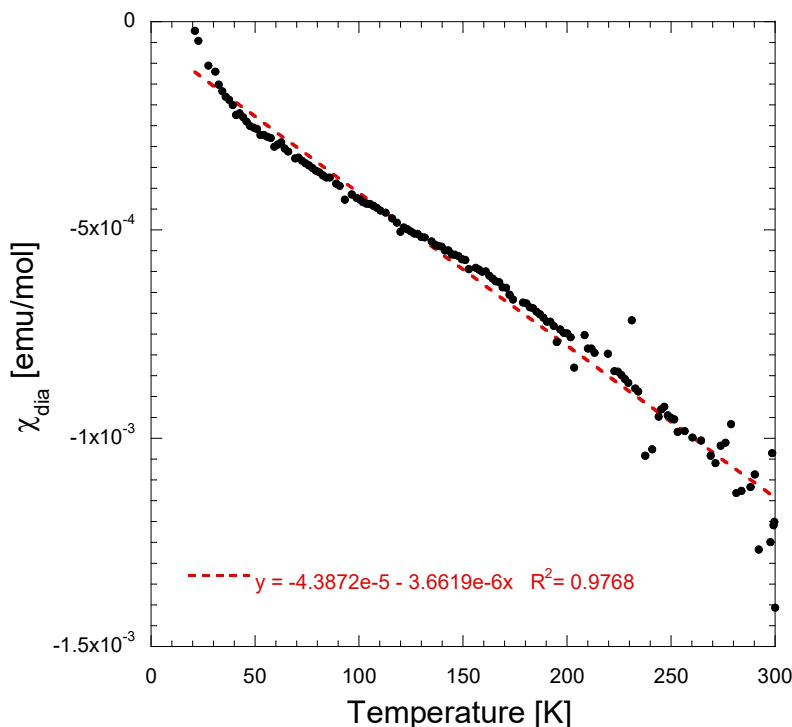


Figure S1. Diamagnetic susceptibility plot of **SQ₂Th** collected by SQUID magnetometry. As shown, the data fits to a linear fit with a negative slope, indicative of diamagnetism within 5 to 300 K. Attempts at fitting this to the HDVV Hamiltonian yielded no fits that would reasonably indicate paramagnetism.

Electronic Absorption Spectroscopy.

An Oxford Instruments Optistat CF Cryostat was suspended in a Hitachi U-4100 Spectrometer such that the optical windows of the cryostat were centered with respect to the beam path. The background was set then, accounting for the baseline contribution from the windows. Each polystyrene thin film was secured to the end of the sample rod and inserted into the cryostat sample chamber which was then pumped and purged with helium gas. Variable Temperature EAS (4-250K) was performed for all SQ₂-Th_n samples (n = 1-3). Strong temperature dependent effects were observed for SQ₂-Th₃, exhibiting multiple isosbestic points, and slight peak intensity variation for SQ₂-Th₂.

In corroboration with the observed magnetic exchange coupling in SQ₂-Th₃, its temperature dependent behavior was rationalized as arriving from thermal population of the accessible singlet and triplet states. The peak intensity of the most intense peaks that are increasing and decreasing with temperature were plotted and normalized iteratively to obtain best fits to the Boltzmann population equation for each state with a single J (2J energy gap) value, -111 cm⁻¹. This result shows good correlation with the value measured from magnetic susceptibility, with deviations likely arising from the differing medium. The spectra of the individual singlet and triplet states were obtained after the realization that at 4K only the singlet state is populated, giving the spectra of the singlet. The singlet spectra was subtracted from the high temperature spectrum weighted by the Boltzmann population determined with the fit J value, the resultant spectra was renormalized with respect to the baseline and represents that of the triplet. As a proof of concept, a range of the VT spectra were reassembled by adding together the component spectra weighted by their predicted Boltzmann populations with remarkable agreement.

The decrease in peak intensity with respect to temperature in SQ₂-Th₂ was initially shelved. After VT EPR and magnetic susceptibility data were obtained and attempts to fit them to a single J-value with a two-state model failed, it was observed that the temperature dependent behavior was observed at a temperature lower than the triplet was occupied as determined by EPR. This combined with our hypothesis of the nature of the changes in the state diagram as a function of Th bridge units lead to the introduction of a three-state model, two singlets and a triplet highest in energy. The absorption peak intensity as a function of temperature and VT EPR intensity were simultaneously fit with identical energy gaps and appropriate expressions for each technique and the relevant state (equations 4 and 5 in text). These energy gaps (306, 822 cm⁻¹) were in good agreement with those determined by fitting the susceptibility to a similar three-state model (317, 959 cm⁻¹. Equation 3).

Single Crystal X-ray Diffraction.

A dark purple/green plate-like specimen of C₁₀₂H₁₁₆B₂N₁₂O₄SZn₂ (SQ₂Th/SQ₂Th) with approximate dimensions 0.23 mm x 0.102 mm x 0.081 mm, was used for X-ray crystallographic analysis. X-ray diffraction data were measured on Bruker D8 Venture PHOTON II CPAD diffractometer equipped with a Cu K α INCOATEC ImuS micro-focus source ($\lambda = 1.54178 \text{ \AA}$). Indexing was performed using APEX4⁶ (Difference Vectors method). Data integration and reduction were performed using SaintPlus.⁷ Absorption correction was performed by multi-scan method implemented in SADABS.⁸ Space group was determined using XPREP implemented in APEX3.⁶ Structure was solved using SHELXT⁹ and refined using SHELXL-2018/3¹⁰ (full-matrix least-squares on F2) through OLEX2 interface program.¹¹ Ellipsoid plot was made with Platon.¹² Disordered parts of SQ₂Th molecule and disordered solvent molecules were refined with restraints. Due to disorder, it was not possible to reliably model hydrogen atoms of isopropanol -OH

groups. The exact amount and orientation of heavily disordered solvent molecules are TENTATIVE! Data and refinement conditions are shown in Table S1, and structure shown in Figure S1.

A dark green plate-like specimen of $C_{106}H_{118}B_2N_{12}O_4S_2Zn_2$ (SQ2Th2/**SQ₂Th₂**) with approximate dimensions 0.506 mm x 0.251 mm x 0.098 mm, was used for X-ray crystallographic analysis. X-ray diffraction data were measured on Bruker D8 Venture PHOTON II CPAD diffractometer equipped with a Cu K α INCOATEC ImuS micro-focus source ($\lambda = 1.54178 \text{ \AA}$). Indexing was performed using APEX4⁶ (Difference Vectors method). Data integration and reduction were performed using SaintPlus.⁷ Absorption correction was performed by multi-scan method implemented in SADABS.⁸ Space group was determined using XPREP implemented in APEX3.⁶ Structure was solved using SHELXT⁹ and refined using SHELXL-2018/3¹⁰ (full-matrix least-squares on F2) through OLEX2 interface program.¹¹ Ellipsoid plot was made with Platon.¹² Disordered solvent molecules were refined with restraints. Due to disorder, it was not possible to reliably model hydrogen atoms of water molecule. The exact amount and orientation of heavily disordered solvent molecules are TENTATIVE! Data and refinement conditions are shown in Table S2, and structure shown in Figure S2.

A dark red plate-like specimen of $C_{110}H_{120}B_2N_{12}O_4S_3Zn_2$ (PDM3-57/**SQ₂Th₃**) with approximate dimensions 0.33 mm x 0.2 mm x 0.1 mm, was used for X-ray crystallographic analysis. data for sample **SQ₂Th₃** were measured on Bruker D8 Venture PHOTON II CPAD diffractometer equipped with a Cu K α INCOATEC ImuS micro-focus source ($\lambda = 1.54178 \text{ \AA}$). Indexing was performed using APEX4⁶ (Difference Vectors method). Data integration and reduction were performed using SaintPlus.⁷ Absorption correction was performed by multi-scan method implemented in SADABS.⁸ Space group was determined using XPREP implemented in APEX3.⁶ Structure was solved using SHELXT⁹ and refined using SHELXL-2018/3¹⁰ (full-matrix least-squares on F2) through OLEX2 interface program.¹¹ Ellipsoid plot was done with Platon.¹² Chloroform molecules are severely disordered, and it was not possible to locate all disordered atoms. The exact amount and positions of chloroform molecules are tentative. Disordered atoms of chloroform and main molecule were refined with restraints. All hydrogen atoms were refined using riding model. Data and refinement conditions are shown in Table S3, and structure (with and without disordered solvent) shown in Figure S3.

Table S1 Crystal data and structure refinement for SQ₂Th.

Identification code	SQ ₂ Th
Empirical formula	C _{108.27} H _{130.18} B ₂ Cl _{2.73} N ₁₂ O _{5.63} SZn ₂
Moiety formula	C ₁₀₂ H ₁₁₆ B ₂ N ₁₂ O ₄ SZn ₂ , 1.635(C ₃ H ₇ O _[Isopropanol]), 1.364(CH ₂ Cl ₂)
Formula weight	1971.01
Temperature/K	100.00
Crystal system	triclinic
Space group	P-1
a/Å	12.3174(6)
b/Å	13.2142(6)
c/Å	33.891(2)
α/°	98.9882(12)
β/°	92.331(2)
γ/°	98.306(2)
Volume/Å ³	5380.1(5)
Z	2
ρ _{calc} /cm ³	1.217
μ/mm ⁻¹	1.795
F(000)	2083.0
Crystal size/mm ³	0.23 × 0.102 × 0.081
Radiation	CuKα (λ = 1.54178)
2θ range for data collection/°	5.29 to 159.724
Index ranges	-15 ≤ h ≤ 15, -16 ≤ k ≤ 16, -43 ≤ l ≤ 43
Reflections collected	157498
Independent reflections	22943 [R _{int} = 0.0520, R _{sigma} = 0.0266]
Data/restraints/parameters	22943/1793/1667
Goodness-of-fit on F ²	1.092
Final R indexes [I ≥ 2σ (I)]	R ₁ = 0.0893, wR ₂ = 0.2304
Final R indexes [all data]	R ₁ = 0.0912, wR ₂ = 0.2313
Largest diff. peak/hole / e Å ⁻³	1.40/-0.70

Table S2 Crystal data and structure refinement for SQ₂Th₂.

Identification code	SQ ₂ Th ₂
Empirical formula	C _{117.02} H _{147.5} B ₂ Cl _{7.14} N ₁₂ O _{9.19} S ₂ Zn ₂
Moiety formula	C ₁₀₆ H ₁₁₈ B ₂ N ₁₂ O ₄ S ₂ Zn ₂ , 3.571(CH ₂ Cl ₂), 3.726(C ₂ H ₆ O), 1.466O _[H₂O]
Formula weight	2338.83
Temperature/K	100.00
Crystal system	triclinic
Space group	P-1
a/Å	11.4225(3)
b/Å	14.9204(4)
c/Å	19.1678(5)
α/°	86.9480(10)
β/°	83.9220(10)
γ/°	73.1760(10)
Volume/Å ³	3108.46(14)
Z	1
ρ _{calc} /cm ³	1.249
μ/mm ⁻¹	2.659
F(000)	1231.0
Crystal size/mm ³	0.506 × 0.252 × 0.098
Radiation	CuKα (λ = 1.54178)
2θ range for data collection/°	4.638 to 160.398
Index ranges	-14 ≤ h ≤ 12, -19 ≤ k ≤ 19, -24 ≤ l ≤ 24
Reflections collected	136799
Independent reflections	13426 [R _{int} = 0.0462, R _{sigma} = 0.0205]
Data/restraints/parameters	13426/255/793
Goodness-of-fit on F ²	1.027
Final R indexes [I ≥ 2σ (I)]	R ₁ = 0.0418, wR ₂ = 0.1154
Final R indexes [all data]	R ₁ = 0.0461, wR ₂ = 0.1194
Largest diff. peak/hole / e Å ⁻³	0.71/-0.67

Table S3 Crystal data and structure refinement for SQ₂Th₃.

Identification code	PDM3_57
Empirical formula	C _{116.41} H _{126.41} B ₂ Cl _{19.23} N ₁₂ O ₄ S ₃ Zn ₂
Moiety formula	C ₁₁₀ H ₁₂₀ B ₂ N ₁₂ O ₄ S ₃ Zn ₂ , 6.408(CHCl ₃)
Formula weight	2687.68
Temperature/K	100.00
Crystal system	triclinic
Space group	P-1
a/Å	13.9530(4)
b/Å	19.5674(5)
c/Å	25.3044(6)
α/°	73.7860(10)
β/°	89.4140(10)
γ/°	76.8000(10)
Volume/Å ³	6448.0(3)
Z	2
ρ _{calc} /cm ³	1.384
μ/mm ⁻¹	5.005
F(000)	2771.0
Crystal size/mm ³	0.33 × 0.2 × 0.1
Radiation	CuKα (λ = 1.54178)
2θ range for data collection/°	4.838 to 159.252
Index ranges	-15 ≤ h ≤ 17, -24 ≤ k ≤ 24, -32 ≤ l ≤ 32
Reflections collected	155286
Independent reflections	27216 [R _{int} = 0.0542, R _{sigma} = 0.0345]
Data/restraints/parameters	27216/2339/1996
Goodness-of-fit on F ²	1.033
Final R indexes [I ≥ 2σ (I)]	R ₁ = 0.0562, wR ₂ = 0.1486
Final R indexes [all data]	R ₁ = 0.0639, wR ₂ = 0.1552
Largest diff. peak/hole / e Å ⁻³	0.80/-0.69

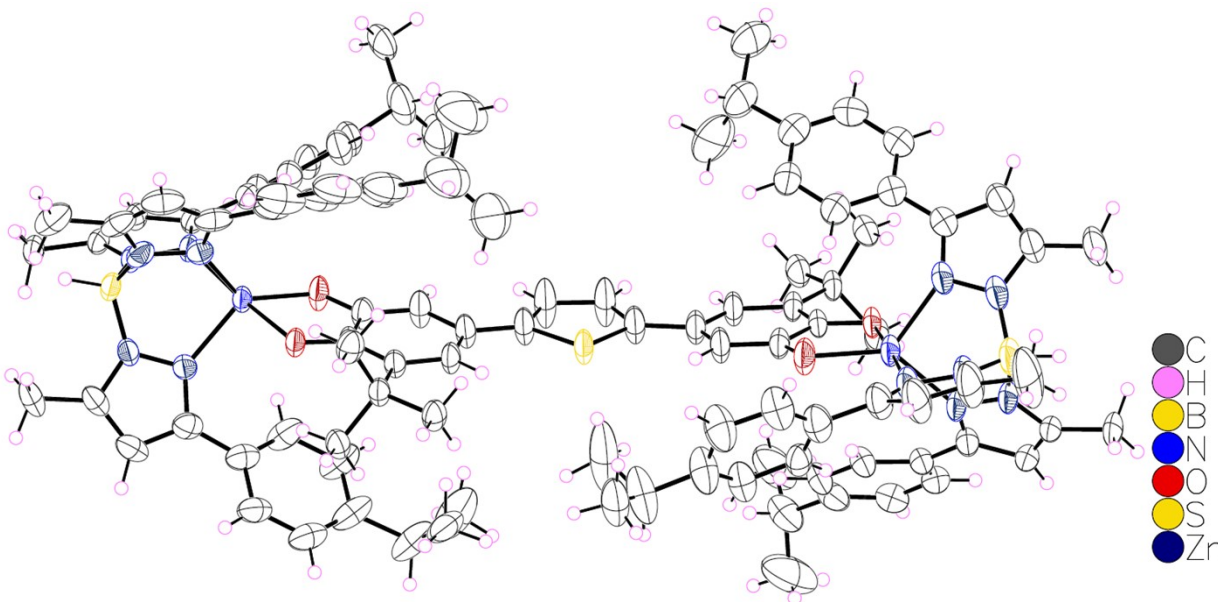


Figure S2. Ellipsoid plot of SQ_2Th molecule. Anisotropic displacement parameters were drawn at 50% probability level. Disordered parts and solvent molecules were omitted for clarity.

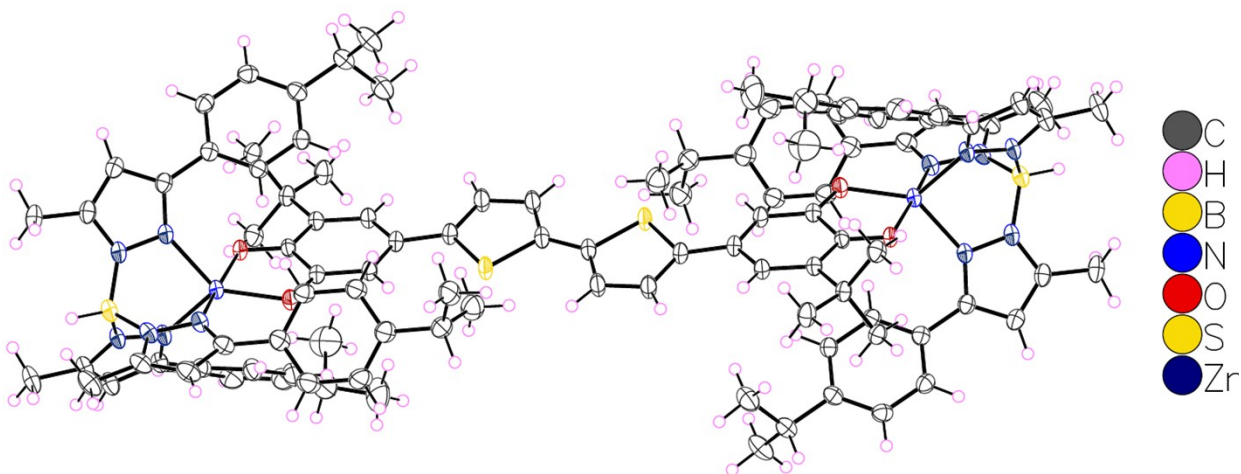
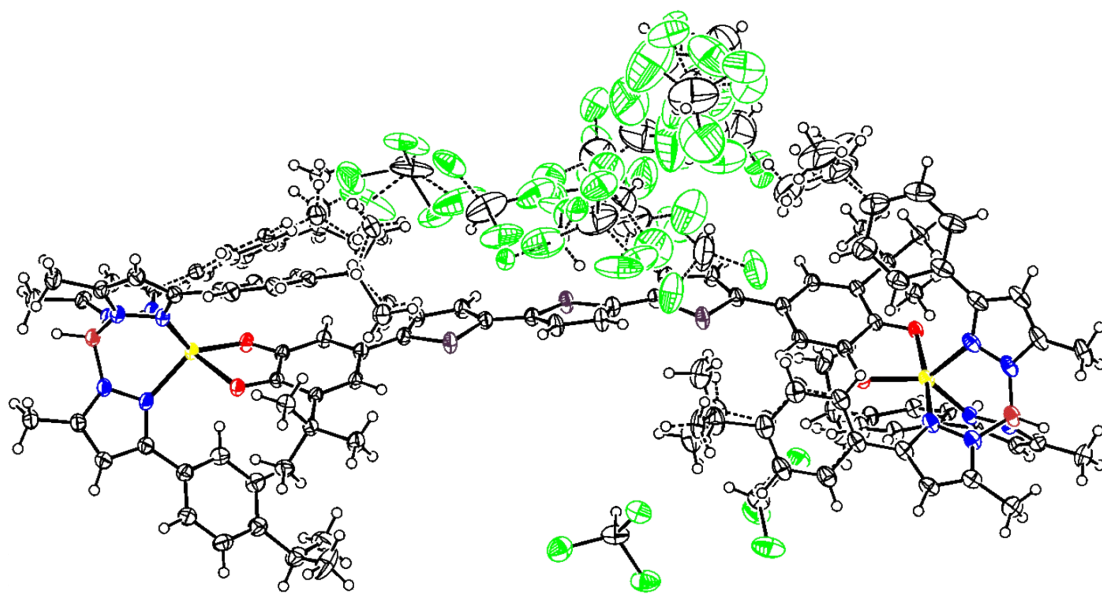
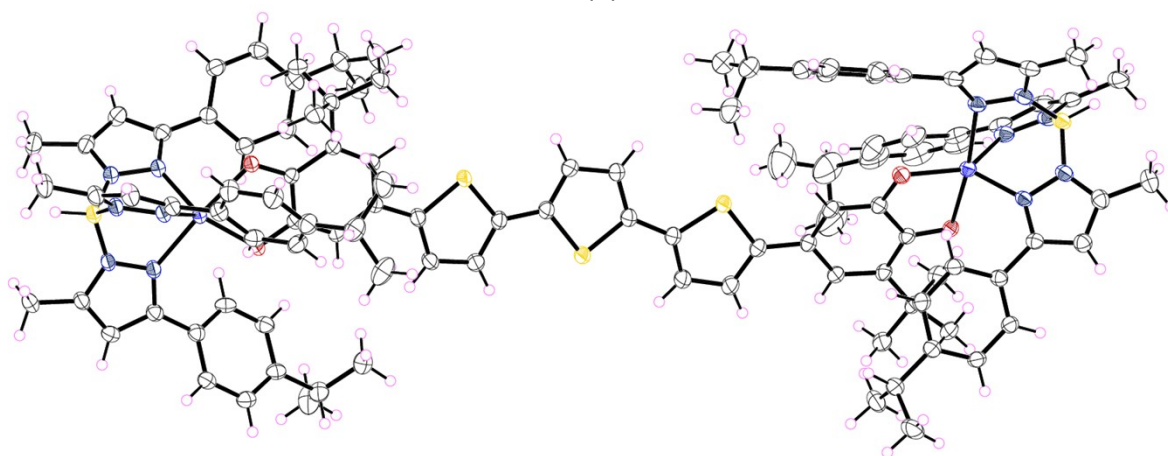


Figure S3. Ellipsoid plot of SQ_2Th_2 molecule. Anisotropic displacement parameters were drawn at 50% probability level. Solvent molecules were omitted for clarity. The molecule is located on inversion center.



(a)



(b)

Figure S4. Ellipsoid plot of SQ_2Th_3 . (a) Asymmetric unit, (b) Main molecule only. 2nd part of disorder was omitted for clarity. Anisotropic displacement parameters were drawn at 50% probability level.

Table S4. Select SQ and Th bond lengths^a for **SQ-SQ** and **SQ-Th₁₋₃-SQ**.

Compound	Dioxolene Bonds	r (Å)	Thiophene Bonds	r (Å)	Dioxolene $\Sigma\Delta_i$ (Å) ^b	Thiophene $\Sigma\Delta_i$ (Å) ^d
SQ-SQ	C1-O1	1.254	---	---	0.198	---
	C2-O2	1.316	---	---		
	C1-C2	1.479	---	---		
	C2-C3	1.370	---	---		
	C3-C4	1.426	---	---		
	C4-C5	1.451	---	---		
	C5-C6	1.362	---	---		
	C6-C1	1.462	---	---		
C4-C4' ^c	1.421	---	---			
SQ-Th-SQ	C1-O1	1.267	C2'-C3'	1.418	0.150	0.110
	C2-O2	1.326	C3'-C4'	1.374		
	C1-C2	1.484				
	C2-C3	1.371				
	C3-C4	1.420				
	C4-C5	1.441				
	C5-C6	1.362				
	C6-C1	1.463				
C4-C2'	1.406					
SQ-Th₂-SQ	C1-O1	1.266	C2'-C3'	1.399	0.119	0.081
	C2-O2	1.308	C3'-C4'	1.389		
	C1-C2	1.476	C4'-C5'	1.395		
	C2-C3	1.377	C5'-C5''	1.412		
	C3-C4	1.404				
	C4-C5	1.438				
	C5-C6	1.368				
	C6-C1	1.452				
C4-C2'	1.422					
SQ-Th₃-SQ	C1-O1	1.268	C2'-C3'	1.383	0.080	0.026
	C2-O2	1.298	C3'-C4'	1.402		
	C1-C2	1.476	C4'-C5'	1.378		
	C2-C3	1.392	C5'-C2''	1.443		
	C3-C4	1.389	C2''-C3''	1.375		
	C4-C5	1.436	C3''-C4''	1.408		
	C5-C6	1.368				
	C6-C1	1.452				
C4-C2'	1.443					

^aAverage values where applicable, see Fig. 2 (in text) for numbering scheme. ^bBond deviation parameter, $\Sigma\Delta_i$ = sum of absolute value of difference in dioxolene bond lengths compared to those of 3,5-di-*tert*-butylsemiquinone.¹³ See text for details. ^cHere, C4-C4' refers to the covalent bond that connects the dioxolene rings. Bond deviation parameters for thiophene bridges determined by comparing the bridges of SQ₂Th, SQ₂Th₂, and SQ₂Th₃ to 2,5-diphenyl-thiophene,¹⁴ 5,5'-diphenyl-2,2'-bithiophene,¹⁵ and 3',4'-dibutyl-5,5''-diphenyl-2,2':5',2''-terthiophene,¹⁶ respectively.^d

Comparison of SQ₂Th and SQ₂Th₂ ¹H-NMR spectra

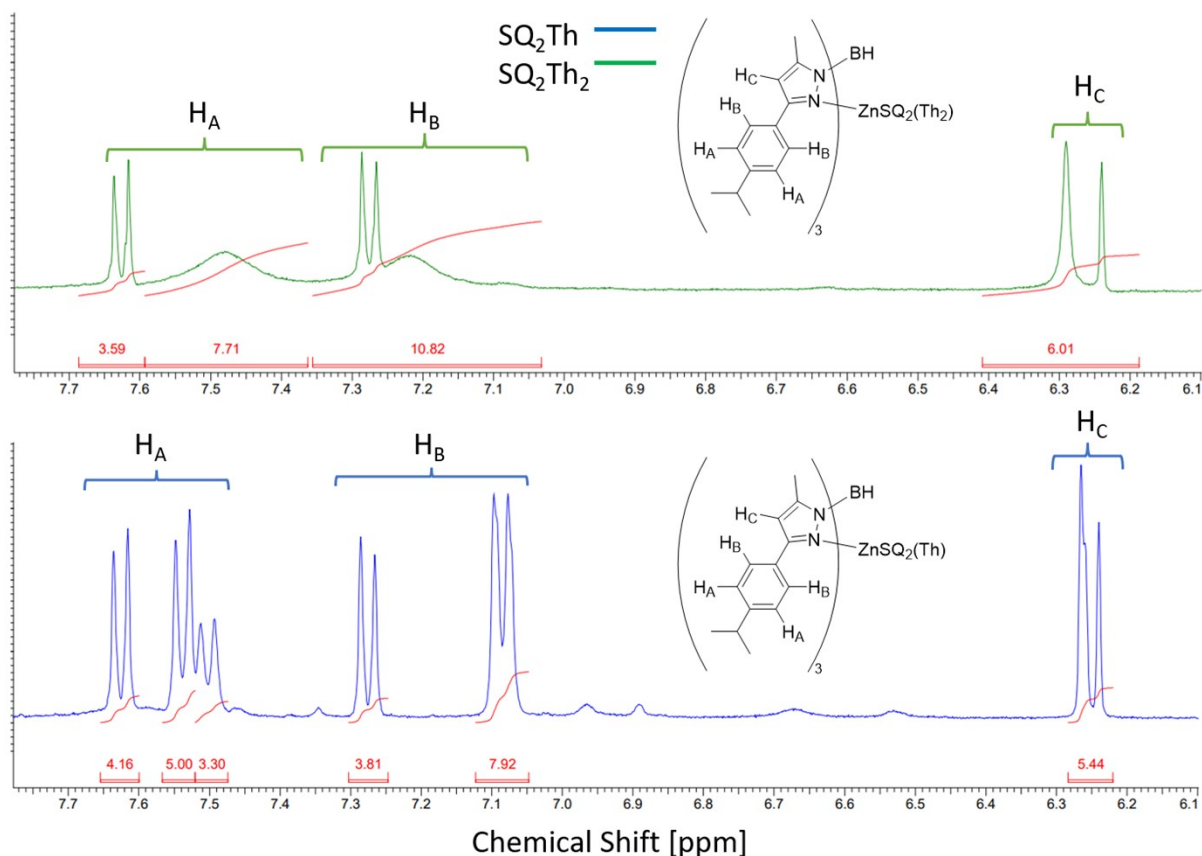


Figure S5. Aromatic regions of the ¹H-NMR spectra of SQ₂Th and SQ₂Th₂ in CD₂Cl₂. Assignments were made by comparing to previously published data on Cum,MeTpZn(OH).¹⁷ SQ₂Th has pronounced aromatic peaks at 7.62 (d; 4 H), 7.54 (d; 5 H), 7.50 (d; 3 H), 7.27 (d; 4 H), 7.08 (d; 8 H) and 6.27 (s; 4 H), 6.24 (s; 2 H). There are a few, broadened signals at 6.96, 6.89, 6.67, and 6.53 ppm that may correspond to different conformers of the thiophene ring relative to Cum,MeTpZnSQ, but otherwise were not identified here. Broadening could be due to the perturbation of the aromaticity by the semiquinone radicals. Notably in the crystal structure shown in **Figure S1**, all of the cumenyl protons in SQ₂Th are roughly 2.5–6 Å away from the semiquinones (in solution free rotation will allow all protons closer proximity) and in relatively close contact with this moiety while the pyrazole protons are all facing away from the semiquinones and 6–7 Å away. If there were substantial degrees of paramagnetism in SQ₂Th, it would be expected for NMR signal dampening to occur for the cumenyl protons substantially and minimally for the pyrazole protons, which there is not for SQ₂Th.^{18, 19} So when analyzing the ¹H-NMR spectra of SQ₂Th₂, there are two broad signals at 7.48 and 7.28 ppm that have been assigned to the cumenyl protons and 2 singlet peaks at 6.29 and 6.24 ppm for the pyrazole protons. These broad signals are indicative of paramagnetic signal dampening due to the open shell nature of SQ₂Th₂ at room temperature. Peaks displaying no paramagnetic broadening for H_A and H_B is likely due to differing conformations that enable the cumenyl groups to be farther away from the semiquinone radical.

REFERENCES

1. Hewitt, P.; Shultz, D. A.; Kirk, M. L., Rules for Magnetic Exchange in Azulene-Bridged Biradicals: quo vadis? *J. Org. Chem.* **2021**, *86*, 15577–15587.
2. Ruf, M.; Vahrenkamp, H., Small Molecule Chemistry of the Pyrazolylborate–Zinc Unit $\text{Tp}^{\text{Cum,Me}}\text{Zn}$. *Inorg. Chem.* **1996**, *35*, 6571–6578.
3. Stoll, S.; Schweiger, A., EasySpin, a comprehensive software package for spectral simulation and analysis in EPR. *J. Magn. Reson.* **2006**, *178*, 42–55.
4. Shultz, D. A.; Fico, R. M., Jr.; Bodnar, S. H.; Kumar, R. K.; Vostrikova, K. E.; Kampf, J. W.; Boyle, P. D., Trends in Exchange Coupling for Trimethylenemethane-Type Bis(Semiquinone) Biradicals and Correlation of Magnetic Exchange with Mixed Valency for Cross-Conjugated Systems. *J. Am. Chem. Soc.* **2003**, *125*, 11761.
5. Kang, B.; Kurutz, J. W.; Youm, K.-T.; Totten, R. K.; Hupp, J. T.; Nguyen, S. T., Catalytically active supramolecular porphyrin boxes: acceleration of the methanolysis of phosphate triesters via a combination of increased local nucleophilicity and reactant encapsulation. *Chem. Sci.* **2012**, *3*, 1938–1944.
6. Bruker APEX4, Bruker AXS LLC: Madison, Wisconsin, USA, 2021.
7. Bruker SAINT V8.40B, Bruker AXS LLC: Madison, Wisconsin, USA.
8. Krause, L.; Herbst-Irmer, R.; Sheldrick, G. M.; Stalke, D., Comparison of silver and molybdenum microfocus X-ray sources for single-crystal structure determination. *J. Appl. Cryst.* **2015**, *48*, 3–10.
9. Sheldrick, G. M., SHELXT - Integrated space-group and crystal-structure determination. *Acta Cryst.* **2015**, *A71*, 3–8.
10. Sheldrick, G. M., Crystal structure refinement with SHELXL. *Acta Cryst.* **2015**, *C71*, 3–8.
11. Dolomanov, O. V.; Bourhis, L. J.; Gildea, R. J.; Howard, J. A. K.; Puschmann, H., OLEX2: A complete structure solution, refinement and analysis program. *J. Appl. Cryst.* **2009**, *42*, 339–341.
12. Spek, A. L., The Program PLATON is designed as a Multipurpose Crystallographic Tool, 1980–2021. *Acta Cryst.* **2020**, *E76*, 1–11.
13. Bodnar, S. H.; Caneschi, A.; Dei, A.; Shultz, D. A.; Sorace, L., A bis-bidentate dioxolene ligand induces thermal hysteresis in valence tautomerism interconversion processes. *Chem. Commun.* **2001**, 2150–2151.
14. Pouzet, P.; Erdelmeier, I.; Ginderow, D.; Dansette, P. M.; Mansuy, D.; Mornon, J.-P., Comparison of the Crystal Structures and Thiophene Ring Aromaticity of 2,5-Diphenylthiophene, Its Sulfoxide and Sulfone. *J. Heterocycl. Chem.* **1997**, *34*, 1567–1574.
15. Akai, R.; Oka, K.; Nishida, R.; Tohnai, N., Systematic Arrangement Control of Functional Organic Molecules. *CrystEngComm* **2022**, *24*, 4180–4186.
16. Graf, D. D.; Duan, R. G.; Campbell, J. P.; Miller, L. L.; Mann, K. R., From Monomers to p-Stacks. A Comprehensive Study of the Structure and Properties of Monomeric, p-Dimerized, and p-Stacked Forms of the Cation Radical of 3',4'-Dibutyl-2,5''-diphenyl-2,2':5',2''-terthiophene. *J. Am. Chem. Soc.* **1997**, *119*, 5888–5899.
17. Ruf, M.; Weis, K.; Vahrenkamp, H., A New Pyrazolylborate Zinc Hydroxide Complex Capable of Cleaving Esters, Amides and Phosphates. *J. Chem. Soc., Chem. Commun.* **1994**, 135–136.
18. Rogawski, R.; Sergeyev, I. V.; Zhang, Y.; Tran, T. H.; Li, Y.; Tong, L.; McDermott, A. E., NMR Signal Quenching from Bound Biradical Affinity Reagents in DNP Samples. *J. Phys. Chem. B* **2017**, *121*, 10770–10781.
19. Softley, C. A.; Bostock, M. J.; Popowicz, G. M.; Sattler, M., Paramagnetic NMR in Drug Discovery. *J. Biomol. NMR* **2020**, *74*, 287–309.